

# Effect of Logarithmic Mesonic Potential on Nucleon Magnetic Moments and Hedgehog Mass

M. Abu-Shady

Received: 4 February 2008 / Accepted: 17 June 2008 / Published online: 12 July 2008  
© Springer Science+Business Media, LLC 2008

**Abstract** The logarithmic mesonic potential is proposed for computing some nucleon properties. The logarithmic potential is based on some aspects of QCD. The field equations have been solved in mean-field approximation. Good results are obtained for the nucleon magnetic moment and the hedgehog mass in comparison with the Skyrmion model. In particular, nucleon properties are calculated for sigma and quark masses which are computed recently.

**Keywords** Mean-field approximation · Nucleon magnetic moments · Linear sigma model

## 1 Introduction

It is widely believed that quantum chromodynamics (QCD) is the fundamental theory underlying strong interaction and the description of the related processes is very difficult due to its non-Abelian color and flavor structures and strong coupling constants. Thus effective models, like the linear sigma model, are constructed in such a way as to respect general properties from the more fundamental theory, such as chiral symmetry and its spontaneous symmetry breaking [1, 2]. Gell-Mann and Levy's linear sigma model [2] is a principal example of spontaneous symmetry breaking (SSB). SSB plays an important role in modeling low energy hadronic physics. The original Gell-Mann and Levy's linear sigma model, after replacing nucleons by quarks [3–9], has been used to describe the binding mechanism of quarks inside baryons and produce quite successful phenomenologies of baryons. Birse and Banerjee [3] constructed equations of motion treating both the  $\sigma$  and  $\pi$ -fields as time-independent classical fields and the quarks and pions in the hedgehog spinor state. A similar model has been reconsidered by Broniowski and Banerjee [4] with numerical errors which

---

M. Abu-Shady (✉)  
Department of Mathematics, Faculty of Science, Menoufia University, Shebin Elkom, Egypt  
e-mail: [abu\\_shady\\_1999@yahoo.com](mailto:abu_shady_1999@yahoo.com)

*Present address:*

M. Abu-Shady  
Institute of Theoretical Physics, University of Tübingen, 72076 Tübingen, Germany

have been corrected in [3]. Birse [5] generalized this mean-field to include angular momentum and isospin projections. Goeke et al. [6] investigated hadron properties in a chiral model for the nucleon based on the linear sigma model with scalar-isoscalar and scalar-isovector mesons coupled to quarks and they used the coherent pair approximation. That work has been reexamined by Aly et al. [7, 8]. They corrected some misprints of the work of Goeke et al. [6], to improve the results in mean-field approximation.

In recent years, there has been growing interest in studying nucleon properties. Some modifications have been suggested in the linear sigma model in the frame of aspects of QCD; Broniowski and Golli [9] analyzed a particular extension of the linear sigma model coupled to valence quarks, which contained an additional term with two gradients of the chiral fields and investigated the dynamic consequences of this term and its relevance to the phenomenology of soliton models of the nucleon. Dmitrasinovic and Myhrer [10] used an extended linear sigma model [11], for which a pair of extra terms is added to the original linear sigma model in order to improve pion-nucleon scattering and the nucleon sigma term. In the same direction, Rashdan et al. [12–14] considered higher-order mesonic interactions in the linear sigma model by using mean-field approximation to better describe nucleon properties.

In the direction of nuclear matter, higher-order mesonic interactions are considered in the framework of the chiral sigma model to get a better description of nuclear matter properties, such as the nuclear matter saturation density and binding energy (for details, see [15–18]). Also, Tsubakihara and Ohnishi [19] derived the logarithmic potential, which is based on some aspects of QCD, to examine nuclear matter properties in comparison with other models.

The aim of this paper is to examine the effect of the logarithmic mesonic potential on nucleon magnetic moments and hedgehog mass for different values of quark and sigma masses which have been computed recently in [20, 21].

This paper is organized as follows. In Sect. 2, the linear sigma model with logarithmic potential is explained briefly. Numerical calculations and discussion of the results are presented in Sect. 3.

## 2 Chiral Quark Sigma Model with Logarithmic Potential

### 2.1 The Linear Sigma Model

In this subsection, we summarize the original linear sigma model of Gell-Mann and Levy [2] and Birse and Banerjee [3]. Logarithmic mesonic potential will be discussed in the next subsection.

The Lagrangian density of the linear sigma model which describes the interactions between quarks via the  $\sigma$ - and  $\pi$ -mesons is written as [3]

$$L(r) = i\bar{\Psi}\gamma_{\mu}\partial^{\mu}\Psi + \frac{1}{2}(\partial_{\mu}\sigma\partial^{\mu}\sigma + \partial_{\mu}\boldsymbol{\pi}\cdot\partial^{\mu}\boldsymbol{\pi}) + g\bar{\Psi}(\sigma + i\gamma_5\boldsymbol{\tau}\cdot\boldsymbol{\pi})\Psi - U_1(\sigma, \boldsymbol{\pi}), \quad (1)$$

with

$$U_1(\sigma, \boldsymbol{\pi}) = \frac{\lambda^2}{4}(\sigma^2 + \boldsymbol{\pi}^2 - v^2)^2 + m_{\pi}^2 f_{\pi}\sigma, \quad (2)$$

is the meson-meson interaction potential where  $\Psi$ ,  $\sigma$  and  $\boldsymbol{\pi}$  are the quark, sigma and pion fields, respectively. In the mean-field approximation, the meson fields are treated as time-independent classical fields. This means that we are replacing powers and products of the meson fields by corresponding powers and products of their expectation values.

The meson-meson interactions in (2) leads to hidden chiral  $SU(2) \times SU(2)$  symmetry with  $\sigma(r)$  taking on a vacuum expectation value

$$\langle \sigma \rangle = -f_\pi, \tag{3}$$

where  $f_\pi = 93$  MeV is the pion decay constant. The final term in (2) is included to break the chiral symmetry. It leads to partial conservation of axial-vector isospin current (PCAC). The parameters  $\lambda^2, v^2$  can be derived in terms of  $f_\pi$  and the masses  $\sigma$ - and  $\pi$ -mesons. One expands the vacuum field expectation values which minimize potential about  $\sigma = -f_\pi, \pi = 0$  we get,

$$v^2 = f_\pi^2 - \frac{m_\pi^2}{\lambda^2} \tag{4}$$

and

$$\lambda^2 = \frac{m_\sigma^2 - m_\pi^2}{2f_\pi^2}. \tag{5}$$

### 2.2 Logarithmic Potential

In this subsection, we explain the physical meaning of the logarithmic potential. We have the following form of the mesonic potential [19]

$$U_2(\sigma, \pi) = \lambda_1^2(\sigma^2 + \pi^2) - \lambda_2^2 \log(\sigma^2 + \pi^2) + m_\pi^2 f_\pi \sigma, \tag{6}$$

is the logarithmic mesonic potential, where  $\Psi, \sigma$  and  $\pi$  are the quark, sigma and pion fields, respectively. It clear that the first and second terms verify the chiral symmetry. Since, there is no parity of the proton and the proton is not massless, the chiral symmetry must be broken. So, the third term in (6) is included to explicitly break the chiral symmetry which, leads to a dynamical mass for quarks and thus nucleon mass [22, 23].

In the case of massless Goldstone bosons,  $m_\pi \simeq 0$ . In fact, the pions are very light, not massless particles. In this case, we have minimum value for the logarithmic potential at a finite value of sigma mass ( $\sigma \simeq -f_\pi$ ). Thus, the potential is shifted from the singularity which comes from the logarithmic term (see Fig. 1).

The parameters  $\lambda_1^2, \lambda_2^2$  are expressed in terms of  $f_\pi$  and the masses  $\sigma$ - and  $\pi$ -mesons

$$\lambda_1^2 = \frac{1}{4}(m_\sigma^2 + m_\pi^2), \tag{7}$$

$$\lambda_2^2 = \frac{f_\pi^2}{4}(m_\sigma^2 - m_\pi^2) \tag{8}$$

(for details see [19]).

Now we expand the extremum, with the shifted field defined as

$$\sigma = \sigma' - f_\pi, \tag{9}$$

substituting (9) into (1, 6), we get

$$L(r) = i\bar{\Psi}\gamma_\mu\partial^\mu\Psi + \frac{1}{2}(\partial_\mu\sigma'\partial^\mu\sigma' + \partial_\mu\pi.\partial^\mu\pi) - g\bar{\Psi}f_\pi\Psi + g\bar{\Psi}\sigma'\Psi + ig\bar{\Psi}\gamma_5\tau.\pi\Psi - U_2(\sigma', \pi) \tag{10}$$

with

$$U_2(\sigma', \boldsymbol{\pi}) = \lambda_1^2((\sigma' - f_\pi)^2 + \boldsymbol{\pi}^2) - \lambda_2^2 \log((\sigma' - f_\pi)^2 + \boldsymbol{\pi}^2) + m_\pi^2 f_\pi (\sigma' - f_\pi).$$

The time-independent fields  $\sigma'(r)$  and  $\pi(r)$  satisfy the Euler-Lagrange equation, and the quark wave function satisfies the Dirac eigenvalue equation [24]. The meson field equations are derived as in [12]

$$\square \sigma' = g \bar{\Psi} \Psi - 2\lambda_1^2(\sigma' - f_\pi) + \frac{2\lambda_2^2(\sigma' - f_\pi)}{((\sigma' - f_\pi)^2 + \boldsymbol{\pi}^2)} - m_\pi^2 f_\pi, \tag{11}$$

$$\square \boldsymbol{\pi} = i g \bar{\Psi} \boldsymbol{\gamma}_5 \cdot \boldsymbol{\tau} \Psi - 2\lambda_1^2 \boldsymbol{\pi} + \frac{2\lambda_2^2 \boldsymbol{\pi}}{((\sigma' - f_\pi)^2 + \boldsymbol{\pi}^2)}, \tag{12}$$

where  $\boldsymbol{\tau}$  refers to Pauli isospin matrices and  $\boldsymbol{\gamma}_5 = \begin{pmatrix} 0 & 1 \\ 1 & 0 \end{pmatrix}$ .

We used the hedgehog ansatz [3] where

$$\boldsymbol{\pi}(r) = \hat{\mathbf{r}} \pi(r). \tag{13}$$

The Dirac equation for the quarks is [12]

$$\frac{du}{dr} = -p(r)u + (W - m_q + S(r))w, \tag{14}$$

where  $S(r) = g\langle\sigma'\rangle$ ,  $P(r) = \langle\boldsymbol{\pi} \cdot \hat{\mathbf{r}}\rangle$  and  $W$  are the scalar potential, the pseudoscalar potential and the eigenvalue of the quarks spinor  $\Psi$ , respectively.

$$\frac{dw}{dr} = -(W - m_q + S(r))u + \left(\frac{2}{r} - p(r)\right)w. \tag{15}$$

Including the color degrees of freedom, one has  $g\bar{\Psi}\Psi$  which becomes  $N_c g\bar{\Psi}\Psi$  where  $N_c = 3$  colors and  $g$  is the coupling constant. The Dirac wave functions  $\Psi(r)$  and  $\bar{\Psi}(r)$  are given by

$$\Psi(r) = \frac{1}{\sqrt{4\pi}} \begin{bmatrix} u(r) \\ iw(r) \end{bmatrix} \quad \text{and} \quad \bar{\Psi}(r) = \frac{1}{\sqrt{4\pi}} [u(r) \quad iw(r)] \tag{16}$$

and the sigma, pion and vector densities are given by

$$\rho_s = N_c g \bar{\Psi} \Psi = \frac{3g}{4\pi} (u^2 - w^2), \tag{17}$$

$$\rho_p = i N_c g \bar{\Psi} \boldsymbol{\gamma}_5 \boldsymbol{\tau} \Psi = \frac{3}{4\pi} g (-2uw), \tag{18}$$

$$\rho_v = \frac{3g}{4\pi} (u^2 + w^2). \tag{19}$$

The boundary conditions for the asymptotics for sigma and pion fields are:

$$\sigma(r) \sim -f_\pi, \quad \pi(r) \sim 0, \quad \text{at } r \rightarrow \infty \tag{20}$$

### 3 Numerical Calculations

#### 3.1 The Scalar Field $\sigma'$

To solve (11), we integrate a suitable Green’s function over the source fields [25]. Thus

$$\sigma'(\mathbf{r}) = \int d^3\mathbf{r}' D_\sigma(\mathbf{r} - \mathbf{r}') \left( g\rho_s(\mathbf{r}') - 2\lambda_1^2(\sigma' - f_\pi) + \frac{2\lambda_2^2(\sigma' - f_\pi)}{((\sigma' - f_\pi)^2 + \pi^2)} - m_\pi^2 f_\pi \right), \tag{21}$$

where

$$D_\sigma(\mathbf{r} - \mathbf{r}') = \frac{1}{4\pi|\mathbf{r} - \mathbf{r}'|} \exp(-m_\sigma|\mathbf{r} - \mathbf{r}'|),$$

the scalar field is spherical in this model as we only need the  $l = 0$  term

$$D_\sigma(\mathbf{r} - \mathbf{r}') = \frac{1}{4\pi} \sinh(m_\sigma r_{<}) \frac{\exp(-m_\sigma r_{>})}{r_{>}}, \tag{22}$$

therefore we arrive at the integral equation for  $\sigma'(\mathbf{r})$ :

$$\begin{aligned} \sigma'(\mathbf{r}) = m_\sigma \int_0^\infty r'^2 dr' & \left( \frac{\sinh(m_\sigma r_{>}) \exp(-m_\sigma r_{>})}{m_\sigma r_{>}} \right) \\ & \times \left( g\rho_s(\mathbf{r}') - 2\lambda_1^2(\sigma' - f_\pi) + \frac{2\lambda_2^2(\sigma' - f_\pi)}{((\sigma' - f_\pi)^2 + \pi^2)} - m_\pi^2 f_\pi \right). \end{aligned} \tag{23}$$

We will solve this equation by iterating to self-consistency.

#### 3.2 The Pion Field $\pi$

To solve (12) we integrate a suitable Green’s function over the source fields. We use  $l = 1$  component of the pion Green’s function. Thus

$$\begin{aligned} \pi(r) = m_\pi \int_0^\infty r'^2 dr' & \frac{[-\sinh(m_\pi r_{<}) + m_\pi r_{<} \cosh(m_\pi r_{<})]}{(m_\pi r_{>})^2} \\ & \times \left( g\rho_p(\mathbf{r}') - 2\lambda_1^2\pi + \frac{2\lambda_2^2\pi}{((\sigma' - f_\pi)^2 + \pi^2)} \right). \end{aligned} \tag{24}$$

We have solved Dirac equations (14, 15) using the fourth-order Rung Kutta method. Due to the implicit nonlinearity of (11, 12), it is necessary to iterate the solution until self-consistency is achieved. To start this iteration process, we use the chiral circle form for the meson fields [12]

$$S(r) = m_q(1 - \cos \theta), \quad P(r) = -m_q \sin \theta, \tag{25}$$

where  $\theta = \tanh r$  and  $m_q$  is the quark mass.

#### 3.3 Calculations of Nucleon Properties

The energy density  $\varepsilon$  is given by [12]

$$\varepsilon = T^{00} = \frac{\partial L}{\partial(\partial_0\Phi_i)} \partial_0\Phi_i - L \tag{26}$$

where  $T^{00}$  can be written as

$$T^{00} = i\bar{\Psi}\partial^0\gamma^0\Psi + \partial_0\sigma'\partial^0\sigma' + \partial_0\boldsymbol{\pi} \cdot \partial^0\boldsymbol{\pi} - \left[ \bar{\Psi}i\gamma^\mu\partial_\mu\Psi - gf_\pi\bar{\Psi}\Psi \right. \\ \left. + igf_\pi\bar{\Psi}\gamma^5\boldsymbol{\tau}\Psi\cdot\boldsymbol{\pi} + g\bar{\Psi}\Psi\sigma' + \frac{1}{2}(\partial_\mu\sigma')^2 + \frac{1}{2}(\partial_\mu\boldsymbol{\pi})^2 - U_2(\sigma', \boldsymbol{\pi}) \right], \quad (27)$$

so

$$\varepsilon = -\bar{\Psi}(i\nabla\cdot\boldsymbol{\gamma} + m_q)\Psi + \frac{1}{2}(\nabla\sigma')^2 + \frac{1}{2}(\nabla\cdot\boldsymbol{\pi})^2 \\ - g\bar{\Psi}(i\gamma_5\boldsymbol{\tau}\cdot\boldsymbol{\pi} + \sigma')\Psi + U_2(\sigma', \boldsymbol{\pi}) - U_2(\sigma' = 0, \boldsymbol{\pi} = 0), \quad (28)$$

which represents quark,  $\sigma'$  and  $\boldsymbol{\pi}$  kinetic energy, quark-meson and meson-meson interaction terms, respectively.

The kinetic energy terms for quark can be reexpressed via the Dirac eigenvalue equation of motion

$$(K.E)_{quark} = -(m_q - S(r))\rho_s(r) + W\rho_v(r) + P(r)\rho_p(r). \quad (29)$$

We use the equation of motion for scalar  $\sigma'$

$$(\square + m_\sigma^2)\sigma' = g\bar{\Psi}\Psi - \frac{\partial U_2}{\partial\sigma'}, \quad (30)$$

thus

$$(K.E)_{sigma} = \frac{1}{2}\sigma' \left[ g\bar{\Psi}\Psi - \frac{\partial U_2}{\partial\sigma'} - m_\sigma^2\sigma' \right]. \quad (31)$$

Similarly for the pion field, we have

$$(K.E)_{pion} = \frac{1}{2}\boldsymbol{\pi} \left[ g\bar{\Psi}i\gamma_5\Psi - \frac{\partial U_2}{\partial\boldsymbol{\pi}} - m_\pi^2\boldsymbol{\pi} \right]. \quad (32)$$

The meson static energy is given by

$$E_{static} = U_2(\sigma', \boldsymbol{\pi}) - U_2(\sigma' = 0, \boldsymbol{\pi} = 0). \quad (33)$$

The sigma-quark interaction energy and the sigma-pion interaction energy are given respectively by

$$(m_q - g\sigma')\rho_s \quad \text{and} \quad -g\boldsymbol{\pi}\rho_p. \quad (34)$$

Finally

$$E_{total} = \int d^3r\varepsilon(r) \\ = N_c W + 4\pi \int_0^\infty r^2 dr\varepsilon(r). \quad (35)$$

(For details of the calculation of the nucleon magnetic moment, see Appendix A.)

### 4 Discussion of Results

The field equations (11 → 15) have been solved by iteration as in [12, 13] for different values of quark and sigma masses. The nucleon observables calculated for  $m_q = 400, 420, 440,$  and  $460$  MeV, sigma mass ( $m_\sigma \geq 200$  MeV, respectively.

From Tables 1–4, the value of hedgehog mass  $M_B$  decreases by increasing the quark mass. This is due to the increase in the attractive interaction between the quarks and meson fields. The dependence on  $m_\sigma$  is much weaker: the nucleon energy ranges from 1047 to 1207 MeV as  $m_\sigma$  is changed from 200 to 1200 MeV (with  $m_q = 460$  MeV).

By using the logarithmic potential, results are obtained for reasonable values of quark masses in the range (400–482.7) MeV which are consistent with NJL model as in [20]. Better results are obtained at  $m_q = 482.7$  MeV and  $m_\sigma = 441$  MeV which has a sigma mass consistent with [21]. In comparison with the free Skyrmion model [26], the nucleon observables are improved. The new model also provides improved observables in comparison

**Table 1** Values of magnetic moments of nucleon and hedgehog mass  $M_B$ . At  $m_q = 400$  MeV. All quantities are in MeV

$m_\sigma$ (MeV)	200	400	600	800	1000	1200
Hedgehog mass $M_B$	1081	1190	1246	1278	1289	1311
Total moment proton $\mu_p(N)$	2.77	2.64	2.637	2.66	2.685	2.707
Total moment neutron $\mu_n(N)$	-1.98	-1.96	-2.00	-2.046	-2.083	-2.113

**Table 2** Values of magnetic moments of nucleon and hedgehog mass  $M_B$ . At  $m_q = 420$  MeV. All quantities are in MeV

$m_\sigma$ (MeV)	200	400	600	800	1000	1200
Hedgehog mass $M_B$	1076	1175	1224	1252	1269	1280
Total moment proton $\mu_p(N)$	2.80	2.69	2.696	2.714	2.733	2.749
Total moment neutron $\mu_n(N)$	-2.029	-2.023	-2.062	-2.102	-2.134	-2.159

**Table 3** Values of magnetic moments of nucleon and hedgehog mass  $M_B$ . At  $m_q = 440$  MeV. All quantities are in MeV

$m_\sigma$ (MeV)	200	400	600	800	1000	1200
Hedgehog mass $M_B$	1064	1153	1197	1221	1236	1245
Total moment neutron $\mu_p(N)$	2.845	2.747	2.745	2.758	2.772	2.784
Total moment neutron $\mu_n(N)$	-2.075	-2.076	-2.114	-2.149	-2.177	-2.197

**Table 4** Values of magnetic moments of nucleon and hedgehog mass  $M_B$ . At  $m_q = 460$  MeV. All quantities are in MeV

$m_\sigma$ (MeV)	200	400	600	800	1000	1200
Hedgehog mass $M_B$	1047	1126	1164	1193	1198	1207
Total moment proton $\mu_p(N)$	2.88	2.79	2.788	2.802	2.806	2.814
Total moment neutron $\mu_n(N)$	-2.12	-2.13	-2.177	-2.203	-2.213	-2.23

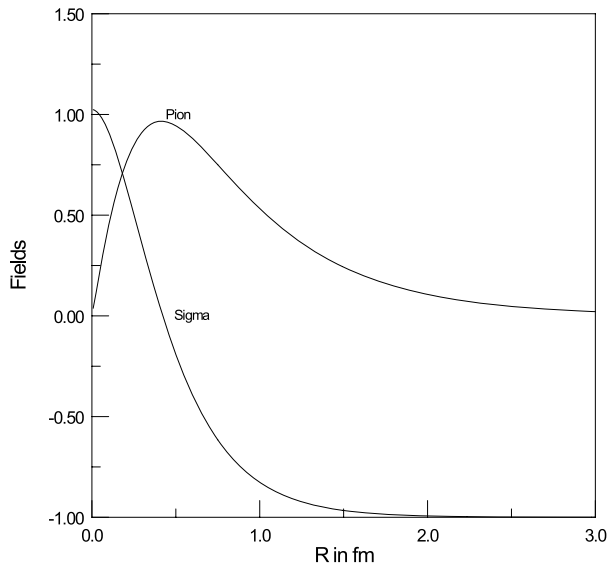
**Table 5** Values of magnetic moments of nucleon and hedgehog mass  $M_B$ . At  $m_\sigma = 441$  MeV. All quantities are in MeV

$m_q$ (MeV)	400	420	440	460	482.7
Hedgehog mass $M_B$	1196	1179	1155	1126	1087
Total moment proton $\mu_p(N)$	2.656	2.712	2.759	2.80	2.85
Total moment neutron $\mu_n(N)$	-1.985	-2.045	-2.098	-2.14	-2.19

**Table 6** Values of nucleon properties are calculated with the Broniowski and Banerjee model [4] and the free Skyrmion model [26] in comparison with the present work

Quantity	[4]	[26]	The present work	Exp. [3]
$M_B$	1119	1944	1087	1086
$\mu_p(N)$	2.87	3.97	2.85	2.79
$\mu_n(N)$	-2.29	-3.30	-2.19	-1.91

**Fig. 1** Sigma and Pion fields in units of  $f_\pi$  as functions of  $R$



with the linear sigma model of Broniowski and Banerjee [4]. They obtained better results at ( $m_q = 500$  MeV,  $m_\sigma = 1200$  MeV), which are the largest masses in comparison with recent works [20, 21]. The results of nucleon magnetic moments are improved in comparison with original linear sigma model [4]. Also, the effect of logarithmic potential is shown on hedgehog mass, where the hedgehog mass is corrected and closed with experimental data (see Table 6).

From Fig. 1, we see that the sigma field passes through zero at  $r = 0.5$ , which we will refer to as the soliton radius ( $r = 0.5$ ), whereas at  $r$  goes to infinity, the pion field goes to zero and the sigma field goes to  $-f_\pi$ . The pion field takes the shape of the P-wave, which gives the attraction of the pion-quark interaction, and goes to zero in a linear manner for large



distances. We also see that the meson fields do not stray far from the circular minimum of the potential ( $\sigma^2 + \pi^2 \simeq f_\pi^2$ ); thus the logarithmic potential has a minimum at a finite  $\sigma$  value so the logarithmic potential is shifted from the singularity which comes from the logarithmic term.

### 5 Conclusion

From the results obtained for the nucleon magnetic moments and hedgehog mass, we see that the mesonic logarithmic potential is successful in giving a good description of nucleon properties. In future work, we need to examine this approach with regard to other nucleon properties.

**Acknowledgement** This work financed by government of Egypt. I would like to thanks Prof. A. Faessler for the hospitality during at my stay at Tübingen university and thanks to Prof. Rashdan.

### Appendix A: Magnetic Moments of the Nucleon

The proton and neutron of the magnetic moments are given by [3]

$$\mu_{n,p} = \left\langle J = I = \frac{1}{2}, M = \frac{1}{2}, I_3 = \pm \frac{1}{2} \left| \int d^3\mathbf{r} \frac{1}{2} \mathbf{r} \times \mathbf{j}_{\epsilon M}(\mathbf{r}) \right| J = I = \frac{1}{2}, M = \frac{1}{2}, I_3 = \pm \frac{1}{2} \right\rangle, \tag{A1}$$

where the electromagnetic current is

$$j_{\epsilon M}(\mathbf{r}) = \bar{\Psi}(\mathbf{r}) \boldsymbol{\gamma} \left( \frac{1}{6} + \frac{\tau_3}{2} \right) \Psi(\mathbf{r}) - \epsilon_{\alpha\beta\gamma} \Phi_\alpha(\mathbf{r}) \nabla \Phi_\beta(\mathbf{r}), \tag{A2}$$

such that

$$(\mathbf{j}_{\epsilon M}(\mathbf{r}))_{nucleon} = \bar{\Psi}(\mathbf{r}) \boldsymbol{\gamma} \left( \frac{1}{6} + \frac{\tau_3}{2} \right) \Psi(\mathbf{r}), \tag{A3}$$

$$(\mathbf{j}_{\epsilon M}(\mathbf{r}))_{meson} = -\epsilon_{\alpha\beta\gamma} \Phi_\alpha(\mathbf{r}) \nabla \Phi_\beta(\mathbf{r}). \tag{A4}$$

#### A.1 Quark Contribution to Magnetic Moment

The vector field  $\mathbf{r}$  can be written as [27]

$$\mathbf{r}_{lm} = r \sqrt{\frac{4\pi}{3}} \sum_m (-)^m Y_{l-m} \hat{e}_m, \quad m = 0, 1, -1, l = 1. \tag{A5}$$

For the dipole magnetic moment calculation we need the quantity

$$\hat{\mathbf{z}} \cdot (\mathbf{r} \times \boldsymbol{\gamma}) = -i\sqrt{2} [r_1 \gamma_1]_{10}, \tag{A6}$$

where

$$[r_1 \gamma_1]_{10} = \sum_{m=\pm 1} \langle 1 \ m \ 1 \ -m \ | \ 1 \ 0 \rangle r_{1m} \gamma_{1-m}, \tag{A7}$$

where the Clebsch-Gordon coefficients are

$$\langle 1\ 1\ 1\ -1\ | 1\ 0 \rangle = \frac{1}{\sqrt{2}}, \tag{A8}$$

$$\langle 1\ -1\ 1\ 1\ | 1\ 0 \rangle = -\frac{1}{\sqrt{2}}; \tag{A9}$$

so

$$\hat{\mathbf{z}} \cdot (\mathbf{r} \times \boldsymbol{\gamma}) = -i\sqrt{\frac{8\pi}{3}} r \gamma_3 [Y_1\sigma_1]_{10}, \tag{A10}$$

where

$$\gamma_1 = \Gamma_3\sigma_1, \quad \Gamma_3 = \begin{pmatrix} 0 & 1 \\ -1 & 0 \end{pmatrix} \tag{A11}$$

and where relevant proton charge matrix element is

$$\langle P\ \uparrow\ | \sum_i \left( \frac{1}{6} + \frac{\tau_3}{2} \right)_i | P\ \uparrow \rangle = +1. \tag{A12}$$

Therefore the magnetic moment becomes

$$\begin{aligned} & \langle \Psi_{l_j, m=j} | \frac{\hat{\mathbf{z}} \cdot (\mathbf{r} \times \boldsymbol{\gamma})}{2} | \Psi_{l_j, m=j} \rangle \\ &= \frac{-i}{2} \sqrt{\frac{8\pi}{3}} \times \langle j, m = j\ 1\ 0\ | j, m = j \rangle \langle \Psi_{l_j} \| r (-i) \gamma_3 [Y_1\sigma_1]_1 \| \Psi_{l_j} \rangle, \end{aligned} \tag{A13}$$

where we have used

$$\langle j\ j\ 1\ 0\ | j\ j \rangle |_{j=\frac{1}{2}} = \left\langle \frac{1}{2}\ \frac{1}{2}\ 1\ 0\ \middle| \frac{1}{2}\ \frac{1}{2} \right\rangle = -\frac{1}{\sqrt{3}}. \tag{A14}$$

In terms of the nuclear magneton, we find

$$\begin{aligned} \frac{\mu}{\mu_{nuc}} &= \frac{1}{3} \sqrt{\frac{8\pi}{3}} m_{nuc} \int_0^\infty dr r^3 \left[ (u(r) w(r) \left\langle 0\ \frac{1}{2}\ \frac{1}{2} \middle\| 1\ \frac{1}{2}\ \frac{1}{2} \right\rangle \right. \\ &\quad \left. \times \left\langle 1\ \frac{1}{2}\ \frac{1}{2} \middle\| [Y_1\sigma_1]_1 \middle\| 0\ \frac{1}{2}\ \frac{1}{2} \right\rangle \right], \end{aligned} \tag{A15}$$

by using reduced matrix element [27], we find

$$\frac{\mu}{\mu_{nuc}} = -\frac{4}{3} m_{nuc} \int_0^\infty dr r^3 u(r) w(r), \tag{A16}$$

therefore

$$\left( \frac{\mu}{\mu_{nuc}} \right)_{neutron} = -\frac{2}{3} \left( \frac{\mu}{\mu_{nuc}} \right)_{proton}. \tag{A17}$$

A.2 Mesonic Contribution to Magnetic Moment

$$\boldsymbol{\mu}_{muc} = \frac{\mathbf{r} \times \mathbf{j}_{mes}}{2}, \tag{A18}$$

$$\mathbf{j}_{mes} = -\epsilon_{\alpha\beta3} \Phi_\alpha \nabla \Phi_\beta, \tag{A19}$$

where  $\Phi_\alpha$  is the pion field with isospin index  $\alpha$ .

$$\hat{\mathbf{Z}} \cdot \left( \frac{\mathbf{r} \times \mathbf{j}_{mes}}{2} \right) = -\epsilon_{\alpha\beta3} \Phi_\alpha \left( \frac{\mathbf{r} \times \nabla}{2} \right) \cdot \hat{\mathbf{Z}} \Phi_\beta, \tag{A20}$$

where  $\hat{\mathbf{Z}}$  is the  $z$ -axis unit vector.

$$\hat{\mathbf{Z}} \cdot \left( \frac{\mathbf{r} \times \mathbf{j}_{mes}}{2} \right) = -\frac{i}{2} \epsilon_{\alpha\beta3} \Phi_\alpha \hat{L}_z \Phi_\beta, \tag{A21}$$

where  $\hat{L}_z$  is the orbital angular momentum in  $z$ -axis.

The hedgehog ansatz for the pion field, we have

$$\Phi_\beta = \hat{\mathbf{r}}_\beta \Phi(r) = \sqrt{\frac{4\pi}{3}} Y_{1\beta}(\hat{\mathbf{r}}) \Phi(r) \tag{A22}$$

and

$$\hat{L}_z \Phi_\beta = \sqrt{\frac{4\pi}{3}} \beta Y_{1\beta}(\hat{\mathbf{r}}) \Phi(r). \tag{A23}$$

Thus

$$\hat{\mathbf{Z}} \cdot \left( \frac{\mathbf{r} \times \mathbf{j}_{mes}}{2} \right) = -\frac{i}{2} \left( \sqrt{\frac{4\pi}{3}} \right)^2 \epsilon_{\alpha\beta3}(\hat{\mathbf{r}}) Y_{1\alpha}(\hat{\mathbf{r}}) \beta Y_{1\beta}(\hat{\mathbf{r}}) \Phi^2(r). \tag{A24}$$

Examine the product of spherical harmonics;

$$\epsilon_{\alpha\beta3} Y_{1\alpha}(\hat{\mathbf{r}}) \beta Y_{1\beta}(\hat{\mathbf{r}}) = -2i (Y_{1+1} Y_{1-1} + Y_{1-1} Y_{1+1}). \tag{A25}$$

From the definition of the spherical harmonics [28], we obtain

$$\left( \frac{\mu}{\mu_{nuc}} \right) = \frac{8\pi}{3} M_{nuc} \int_0^\infty dr r^2 \Phi^2(r). \tag{A26}$$

Including the  $\frac{1}{3}$  projection factor, we get

$$\left( \frac{\mu}{\mu_{nuc}} \right) = \frac{8\pi}{9} M_{nuc} \int_0^\infty dr r^2 \Phi^2(r). \tag{A27}$$

## References

1. Gastorowicz, S., Geffen, D.A.: *Rev. Mod. Phys.* **41**(3) (1969)
2. Gell-Mann, M., Levy, M.: *Nuovo Cimento* **16**, 705 (1960)
3. Birse, M., Banerjee, M.: *Phys. Rev. D* **31**, 118 (1985)
4. Broniowski, W., Banerjee, M.: *Phys. Lett. B* **158**, 335 (1985)
5. Birse, M.: *Phys. Rev. D* **33**, 1934 (1986)
6. Goeke, K., Harve, M., Gru, F., Urbano, J.N.: *Phys. Rev. D* **37**, 754 (1988)
7. Aly, T.S.T., McNeil, J.A., Pruess, S.: *Phys. Rev. D* **60**, 114002 (1999)
8. Aly, T.S.T., Rashdan, M., Abu-Shady, M.: *Int. J. Theor. Phys.* **45**(9), 1654–1658 (2006)
9. Broniowski, W., Golli, B.: *Nucl. Phys. A* **714**, 575–588 (2003)
10. Dmitrasinovic, V., Myhrer, F.: arXiv:[hep-ph/9911320](https://arxiv.org/abs/hep-ph/9911320)
11. Bjorken, J.D., Nauenberg, M.: *Ann. Rev. Nucl. Sci.* **18**, 229 (1968)
12. Rashdan, M., Abu-Shady, M., Ali, T.S.T.: *Int. J. Mod. Phys. E* **15**(1), 143–152 (2006)
13. Rashdan, M., Abu-Shady, M., Ali, T.S.T.: *Int. J. Mod. Phys. A* **22**(14–15), 2673–2681 (2007)
14. Abu-Shady, M., Rashdan, M., Ali, T.S.T.: *Fizika B (Zagrab)* **16**(1), 59–66 (2007)
15. Sahu, P.K., Ohnishi, A.: *Prog. Theor. Phys.* **104**, 1163–1171 (2000)
16. Boguta, J.: *Phys. Lett. B* **120**, 34 (1983)
17. Boguta, J.: *Phys. Lett. B* **128**, 19 (1983)
18. Sahu, P.K., Jha, T.K., Panda, K.C., Patra, S.K.: *Nucl. Phys. A* **733**, 169–184 (2004)
19. Tsubakihara, K., Ohnishi, A.: *Prog. Theor. Phys.* **117**, 903–921 (2007)
20. Rashdan, M.: *Chaos Solitons Fractals* **18**, 107 (2003)
21. Leutwyler, H.: *Int. Mod. Phys. A* **22**, 257–265 (2007)
22. Petropoulos, N.: arXiv:[hep-ph/0402136v1](https://arxiv.org/abs/hep-ph/0402136v1) (2004)
23. Petropoulos, N.: *J. Phys. G* **25**, 2225 (1999). arXiv:[hep-ph/9809383](https://arxiv.org/abs/hep-ph/9809383)
24. Mosel, U.: *Fields, Symmetries and Quarks*. McGraw-Hill, New York (1989)
25. Koonin, S.E., Meredith, D.C.: *Computational Physics (Fortran version)*. Addison Wesley, New York (1990)
26. Braghin, F.L., Cavalcante, I.P.: *Phys. Rev. C* **67**, 065207 (2003)
27. Brink, D.M., Satchler, G.K.: *Angular Momentum*. Oxford University Press, Oxford (1971)
28. Kroemer, H.: *Quantum Mechanics*. Prentice Hall, New York (1944)